

Relationship between the symmetry energy and the single-nucleon potential in isospin-asymmetric nucleonic matter

Chang Xu¹, Bao-An Li², and Lie-Wen Chen³

¹ School of Physics, Nanjing University, Nanjing 210008, China

² Department of Physics and Astronomy, Texas A&M University-Commerce, Commerce, Texas 75429-3011, USA

³ Department of Physics and Astronomy and Shanghai Key Laboratory for Particle Physics and Cosmology, Shanghai Jiao Tong University, Shanghai 200240, China

Received: date / Revised version: date

Abstract. In this contribution, we review the most important physics presented originally in our recent publications [1,2,3,4,5,6]. Some new analyses, insights and perspectives are also provided. We showed recently that the symmetry energy $E_{sym}(\rho)$ and its density slope $L(\rho)$ at an arbitrary density ρ can be expressed analytically in terms of the magnitude and momentum dependence of the single-nucleon potentials by using the Hugenholtz-Van Hove (HVH) theorem. These relationships provide new insights about the fundamental physics governing the density dependence of nuclear symmetry energy. Using the isospin and momentum (k) dependent MDI interaction as an example, the contribution of different terms in the single-nucleon potential to the $E_{sym}(\rho)$ and $L(\rho)$ are analyzed in detail at different densities. It is shown that the behavior of $E_{sym}(\rho)$ is mainly determined by the first-order symmetry potential $U_{sym,1}(\rho, k)$ of the single-nucleon potential. The density slope $L(\rho)$ depends not only on the first-order symmetry potential $U_{sym,1}(\rho, k)$ but also the second-order one $U_{sym,2}(\rho, k)$. Both the $U_{sym,1}(\rho, k)$ and $U_{sym,2}(\rho, k)$ at normal density ρ_0 are constrained by the isospin and momentum dependent nucleon optical potential extracted from the available nucleon-nucleus scattering data. The $U_{sym,2}(\rho, k)$ especially at high density and momentum affects significantly the $L(\rho)$, but it is theoretically poorly understood and currently there is almost no experimental constraints known.

PACS. 21.65.Cd Asymmetric matter, neutron matter – 21.65.Ef Symmetry energy

1 Introduction

In recent years, extensive experimental and theoretical efforts have been devoted to determining the density dependence of nuclear symmetry energy $E_{sym}(\rho)$, which characterizes the isospin dependent part of the equation of state (EOS) of asymmetric nuclear matter [7,8,9]. Starting from a model energy density functional, the symmetry energy $E_{sym}(\rho)$ and its density slope $L(\rho) = 3\rho \frac{\partial E_{sym}(\rho)}{\partial \rho}$ can be easily obtained by expanding the EOS of asymmetric nuclear matter as a power series of isospin asymmetry $\delta = \frac{\rho_n - \rho_p}{\rho_n + \rho_p}$: $E(\rho, \delta) = E_0(\rho) + E_{sym}(\rho)\delta^2 + O(\delta^4)$ where $E_0(\rho)$ is the EOS of symmetric nuclear matter and $E_{sym}(\rho)$ is the so-called symmetry energy. Although much information about the EOS of symmetric nuclear matter $E_0(\rho)$ has been accumulated over the past several decades, our knowledge about the $E_{sym}(\rho)$ is unfortunately still very poor. However, it has been clearly shown in many references that the symmetry energy and its density slope are critical for understanding not only the structure of rare

isotopes and the reaction mechanism of heavy-ion reactions, but also many interesting issues in astrophysics [10, 11, 12, 13, 14, 15, 16, 17, 18, 19, 20, 21]. Thus, to determine the density dependence of $E_{sym}(\rho)$ has now become a major goal in both nuclear physics and astrophysics. While significant progress has been made recently in constraining the $E_{sym}(\rho)$ especially below and around the normal density, see, e.g., [22, 23, 24, 25, 26], much more work needs to be done to constrain the $E_{sym}(\rho)$ at high densities [27, 28, 29, 30, 31, 32, 33, 34, 35, 36, 37, 38, 39, 40, 41]. The present theoretical predictions on the high density behavior of $E_{sym}(\rho)$ are rather diverse by various nonrelativistic/relativistic mean-field approaches, depending closely on the mean-field/single-nucleon potential used in the model.

As an important input for calculations of nuclear structures and simulations of heavy-ion reactions, the single-nucleon potential $U_{n/p}(\rho, \delta, p)$ itself can also be obtained by a functional derivative of the energy density $\xi = \rho E(\rho, \delta)$ with respect to the distribution function [28, 29, 30]. Thus, the single-nucleon potential and the symmetry energy are intrinsically correlated as they can be both obtained from the same energy density functional. In this paper, we will review the direct relationship between the symmetry en-

Send offprint requests to:

ergy and the single-nucleon potential $U_{n/p}(\rho, \delta, p)$ [1,2,3,4,5,6]. For studying the symmetry energy and its density slope, the direct relationship between the single-nucleon potential and the symmetry energy without going through the procedure to construct the corresponding energy density functional is obviously advantageous. This is because one can directly extract both the isoscalar and isovector nucleon optical potentials at saturation density from experimental data, such as (p,n) charge exchange reactions and proton/neutron-nucleus scattering. One can then easily calculate the symmetry energy and its density slope at saturation density directly from the optical potentials without having to first construct the energy density functional [1]. Moreover, to find the relationship between the symmetry energy and the isoscalar and isovector single-nucleon potentials is actually a major goal of the current efforts in developing nuclear energy density functionals [42]. It is also mentioned that, within relativistic covariant formulism, the Lorentz covariant nucleon self-energy decomposition of the nuclear symmetry energy has also been obtained recently [43].

In this paper, we shall firstly recall the general relationship between the symmetry energy and the single-nucleon potential in isospin asymmetric matter derived earlier in Refs. [1,2,5] using the Hugenholtz-Van Hove theorem [44]. The analytical expressions of the symmetry energy $E_{sym}(\rho)$ and its density slope $L(\rho)$ are very helpful in gaining deeper insights into the microscopic origins of $E_{sym}(\rho)$ and $L(\rho)$. Using the isospin and momentum dependent MDI interaction as an example [28,29,30], the contributions of different terms in the single-nucleon potential (MDI) to the $E_{sym}(\rho)$ and $L(\rho)$ are analyzed in details for different densities. The outline of this paper is as follows. In Section 2, the relationship between the symmetry energy and the single-nucleon potential is derived by using the Hugenholtz-Van Hove theorem. In Section 3, the isoscalar and isovector potentials of the isospin and momentum dependent MDI interaction are introduced in details. The first-order and second-order symmetry potentials of the MDI interaction are also compared with those from several microscopic approaches in Section 3. The optical model analysis of the single-nucleon potential and the corresponding symmetry energy and its density slope are presented in Section 4. Finally a brief summary is given in Section 5.

2 Relationship between the symmetry energy and the single-nucleon potential based on the Hugenholtz-Van Hove theorem

In 1958, Hugenholtz and Van Hove proposed a famous theorem on the single particle energy in a Fermi gas with interaction at absolute zero in temperature [44]. In the following, we recall the Hugenholtz-Van Hove theorem and its application in deriving the relation between the nuclear symmetry energy and the single-nucleon potential. The HVH theorem describes a fundamental relation among the Fermi energy E_F , the average energy per particle E and

the pressure of the system P at zero temperature. For a one-component system, in terms of the energy density $\xi = \rho E$, the general HVH theorem can be written as [44,45]

$$E_F = \frac{d\xi}{d\rho} = E + \frac{P}{\rho}. \quad (1)$$

For a special system with zero pressure the Fermi energy E_F is equal to the average energy per particle E of the system.

$$E_F = E. \quad (2)$$

It is stressed that the general HVH theorem of Eq.(1) is valid at arbitrary density as long as the temperature T remains zero [44,45]. It does not depend on the precise nature of the interaction. In fact, a successful theory of nuclear matter is required not only to describe properly the saturation properties of nuclear matter but also to fulfill the HVH theorem at any density. For instance, in the original paper of the HVH theorem [44], Hugenholtz and Van Hove used their theorem to test the internal consistency of the nuclear matter theory of Brueckner. They found the large discrepancy between the values of E_F and E in the Brueckner's theory at equilibrium and pointed out that Brueckner neglected important cluster terms contributing to the single particle energy [44].

According to the HVH theorem, the Fermi energies of neutrons and protons in isospin asymmetric nuclear matter are, respectively [2,3,4,44,45,46,47,48,49],

$$t(k_F^n) + U_n(\rho, \delta, k_F^n) = \frac{\partial \xi}{\partial \rho_n}, \quad (3)$$

$$t(k_F^p) + U_p(\rho, \delta, k_F^p) = \frac{\partial \xi}{\partial \rho_p}, \quad (4)$$

where $t(k) = \hbar k^2/2m$ is the kinetic energy and $U_{n/p}$ is the neutron/proton single-nucleon potential. The Fermi momenta of neutrons and protons are $k_F^n = k_F(1 + \delta)^{1/3}$ and $k_F^p = k_F(1 - \delta)^{1/3}$, respectively. Subtracting Eq.(4) from Eq.(3) gives [46,47,48,49]

$$\begin{aligned} & [t(k_F^n) - t(k_F^p)] + [U_n(\rho, \delta, k_F^n) - U_p(\rho, \delta, k_F^p)] \\ &= \frac{\partial \xi}{\partial \rho_n} - \frac{\partial \xi}{\partial \rho_p}. \end{aligned} \quad (5)$$

The single-nucleon potentials can be expanded as a power series of isospin asymmetry δ while respecting the charge symmetry of nuclear interactions under the exchange of protons and neutrons,

$$\begin{aligned} U_\tau(\rho, \delta, k) &= U_0(\rho, k) + \sum_{i=1,2,3\dots} U_{sym,i}(\rho, k)(\tau\delta)^i \quad (6) \\ &= U_0(\rho, k) + U_{sym,1}(\rho, k)(\tau\delta) + U_{sym,2}(k)(\tau\delta)^2 + \dots \end{aligned}$$

where $\tau=1$ (-1) for neutrons (protons). If one neglects the higher-order terms ($\delta^2, \delta^3, \dots$), Eq.(6) reduces to the so-called Lane potential [50]. Expanding both the kinetic

and potential energies around the Fermi momentum k_F , the left side of Eq.(5) can be further written as

$$\begin{aligned}
& [t(k_F^n) - t(k_F^p)] + [U_n(\rho, \delta, k_F^n) - U_p(\rho, \delta, k_F^p)] \\
&= \sum_{i=1,2,3,\dots} \frac{1}{i!} \frac{\partial^i [t(k) + U_0(\rho, k)]}{\partial k^i} \Big|_{k_F} k_F^i \\
&\times [(\sum_{j=1,2,3,\dots} F(j)\delta^j)^i - (\sum_{j=1,2,3,\dots} F(j)(-\delta)^j)^i] \\
&+ \sum_{l=1,2,3,\dots} U_{sym,l}(\rho, k_F) [\delta^l - (-\delta)^l] \\
&+ \sum_{l=1,2,3,\dots} \sum_{i=1,2,3,\dots} \frac{1}{i!} \frac{\partial^i U_{sym,l}(\rho, k)}{\partial k^i} \Big|_{k_F} k_F^i \\
&\times [(\sum_{j=1,2,3,\dots} F(j)\delta^j)^i \delta^l - (\sum_{j=1,2,3,\dots} F(j)(-\delta)^j)^i (-\delta)^l] \\
&= \left[\frac{2}{3} \frac{\partial [t(k) + U_0(\rho, k)]}{\partial k} \Big|_{k_F} k_F + 2U_{sym,1}(\rho, k_F) \right] \delta + \dots (7)
\end{aligned}$$

where the function $F(j) = \frac{1}{j!} [\frac{1}{3}(\frac{1}{3}-1)\dots(\frac{1}{3}-j+1)]$ is introduced. For the right side of Eq.(5), expanding in powers of δ gives

$$\frac{\partial \xi}{\partial \rho_n} - \frac{\partial \xi}{\partial \rho_p} = 4E_{sym}(\rho)\delta + \mathcal{O}(\delta^3) \quad (8)$$

Comparing the coefficient of each δ^i term in Eq.(7) with that in Eq.(8) then gives the symmetry energy of any order. For instance, we derived the most important quadratic term

$$\begin{aligned}
E_{sym}(\rho) &= \frac{1}{6} \frac{\partial [t(k) + U_0(\rho, k)]}{\partial k} \Big|_{k_F} k_F + \frac{1}{2} U_{sym,1}(\rho, k_F) \\
&= \frac{1}{3} t(k_F) + \frac{1}{6} \frac{\partial U_0}{\partial k} \Big|_{k_F} \cdot k_F + \frac{1}{2} U_{sym,1}(\rho, k_F) (9)
\end{aligned}$$

By adding Eq.(3) and Eq.(4), the following equation is obtained

$$\begin{aligned}
& [t(k_F^n) + t(k_F^p)] + [U_n(\rho, \delta, k_F^n) + U_p(\rho, \delta, k_F^p)] \\
&= \frac{\partial \xi}{\partial \rho_n} + \frac{\partial \xi}{\partial \rho_p}. \quad (10)
\end{aligned}$$

The right side of Eq.(10) can be further written as

$$\begin{aligned}
\frac{\partial \xi}{\partial \rho_n} + \frac{\partial \xi}{\partial \rho_p} &= 2E_0(\rho) + 2\rho \frac{\partial E_0(\rho)}{\partial \rho} \\
&+ \left[\frac{2}{3} L(\rho) - 2E_{sym}(\rho) \right] \delta^2 + \mathcal{O}(\delta^4). \quad (11)
\end{aligned}$$

Expanding again both the kinetic and potential energies in the left side of Eq.(10) around k_F and comparing the corresponding coefficients of two sides in Eq.(10), we obtained the exact analytical equation of the density slope $L(\rho)$

$$\begin{aligned}
L(\rho) &= \frac{1}{6} \frac{\partial [t(k) + U_0(\rho, k)]}{\partial k} \Big|_{k_F} \cdot k_F \\
&+ \frac{1}{6} \frac{\partial^2 [t(k) + U_0(\rho, k)]}{\partial k^2} \Big|_{k_F} \cdot k_F^2 + \frac{3}{2} U_{sym,1}(\rho, k_F) \\
&+ \frac{\partial U_{sym,1}(\rho, k)}{\partial k} \Big|_{k_F} \cdot k_F + 3U_{sym,2}(\rho, k_F). \quad (12)
\end{aligned}$$

Similar to the HVH theorem, the analytical expressions in Eq.(9) and Eq.(12) are valid at any density. The values of both $E_{sym}(\rho)$ and $L(\rho)$ can be easily calculated simultaneously once the single-nucleon potential is known. The most critical advantage of the expressions in Eq.(9) and Eq.(12) is that they allow us to determine the $E_{sym}(\rho)$ and $L(\rho)$ directly from the value and momentum dependence of the single-nucleon potential at ρ . Essentially, this enables one to translate the task of determining the density dependence of the symmetry energy into a problem of finding the momentum dependence of the $U_0(\rho, k)$, $U_{sym,1}(\rho, k)$, and $U_{sym,2}(\rho, k)$.

3 The isoscalar and isovector potentials of the Momentum-Dependent-Interaction (MDI)

Several famous single-nucleon potentials have been widely applied in the transport model simulations for heavy-ion reactions. Usually, these single-nucleon potentials are derived from their corresponding energy density functional that has been carefully adjusted to properties of nuclear matter. To show in details the contribution of each term in Eq.(9) and Eq.(12) to the symmetry energy and its density slope, we use the widely-used Momentum-Dependent-Interaction (MDI) as an example [28,29,30], which is derived from the Hartree-Fock approximation using a modified Gogny effective interaction [51]

$$\begin{aligned}
U_\tau(\rho, \delta, \mathbf{p}) &= A_u(x) \frac{\rho\tau'}{\rho_0} + A_l(x) \frac{\rho\tau}{\rho_0} \\
&+ B \left(\frac{\rho}{\rho_0} \right)^\sigma (1 - x\delta^2) - 4\tau x \frac{B}{\sigma+1} \frac{\rho^{\sigma-1}}{\rho_0^\sigma} \delta\rho_{\tau'} \\
&+ \frac{2C_{\tau,\tau}}{\rho_0} \int d^3p' \frac{f_\tau(\mathbf{r}, \mathbf{p}')}{1 + (\mathbf{p} - \mathbf{p}')^2/\Lambda^2} \\
&+ \frac{2C_{\tau,\tau'}}{\rho_0} \int d^3p' \frac{f_{\tau'}(\mathbf{r}, \mathbf{p}')}{1 + (\mathbf{p} - \mathbf{p}')^2/\Lambda^2}, \quad (13)
\end{aligned}$$

where $\tau = 1(-1)$ for neutrons (protons) and $\tau \neq \tau'$; $\sigma = 4/3$ is the density-dependence parameter; $f_\tau(\mathbf{r}, \mathbf{p})$ is the phase space distribution function at coordinate \mathbf{r} and momentum $\mathbf{p} = \hbar\mathbf{k}$. The parameters $B, C_{\tau,\tau}, C_{\tau,\tau'}$ and Λ are fitted to the nuclear matter saturation properties [28,29,30]. The parameters B and σ in the MDI single-nucleon potential are related to the t_0 and α in the Gogny effective interaction via $t_0 = \frac{8}{3} \frac{B}{\sigma+1} \frac{1}{\rho_0^\sigma}$ and $\sigma = \alpha + 1$ [51]. The parameter x has been introduced to vary the density dependence of the symmetry energy while keep the properties of symmetric nuclear matter unchanged [22,23] and it is related to the spin (isospin)-dependence parameter x_0 via $x = (1 + 2x_0)/3$ [3]. The momentum dependence of the symmetry potential stems from the different strength parameters $C_{\tau,\tau'}$ and $C_{\tau,\tau}$ for a nucleon of isospin τ interacting with unlike and like nucleons. More specifically, $C_{unlike} = -103.4$ MeV while $C_{like} = -11.7$ MeV. The quantities $A_u(x) = -95.98 - x \frac{2B}{\sigma+1}$ and $A_l(x) =$

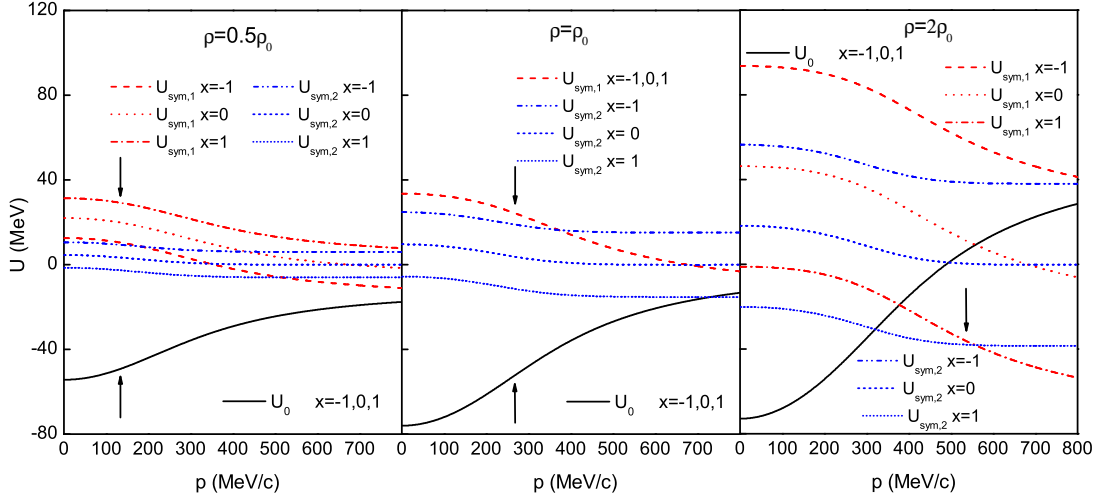


Fig. 1. Momentum dependence of the isoscalar and isovector potentials of the MDI interaction with different x parameters at densities $0.5\rho_0$ (left panel), ρ_0 (middle panel), and $2\rho_0$ (right panel), respectively. The Fermi momentum $p = p_f$ is denoted by the black arrows.

$-120.57 + x \frac{2B}{\sigma+1}$ are parameters. By expanding the single-nucleon potential in δ , the isospin independent isoscalar potential $U_0(\rho, p)$ of the MDI interaction is given by

$$U_0(\rho, p) = \frac{A_l(x) + A_u(x)}{2} \frac{\rho}{\rho_0} + B \left(\frac{\rho}{\rho_0} \right)^\sigma + \frac{2(C_l + C_u)}{\rho_0} \frac{\pi \Lambda^2}{h^3 p} \times \{ 4pp_f + 4p\Lambda \operatorname{Arctan} \left[\frac{p - p_f}{\Lambda} \right] - 4p\Lambda \operatorname{Arctan} \left[\frac{p + p_f}{\Lambda} \right] - (p^2 - p_f^2 - \Lambda^2) \log \left[\frac{(p + p_f)^2 + \Lambda^2}{(p - p_f)^2 + \Lambda^2} \right] \}. \quad (14)$$

The first order symmetry potential of the MDI interaction $U_{sym,1}(\rho, p)$ is

$$U_{sym,1}(\rho, p) = \frac{A_l(x) - A_u(x)}{2} \frac{\rho}{\rho_0} - \frac{2xB}{\sigma+1} \left(\frac{\rho}{\rho_0} \right)^\sigma + \frac{2(C_l - C_u)}{\rho_0} \frac{2\pi \Lambda^2 p_f^2}{3h^3 p} \times \log \left[\frac{(p + p_f)^2 + \Lambda^2}{(p - p_f)^2 + \Lambda^2} \right]. \quad (15)$$

The second order symmetry potential of the MDI interaction $U_{sym,2}(\rho, p)$ is

$$U_{sym,2}(\rho, p) = -x B \left(\frac{\rho}{\rho_0} \right)^\sigma + \frac{2xB}{\sigma+1} \left(\frac{\rho}{\rho_0} \right)^\sigma + \frac{2(C_l + C_u)}{\rho_0} \frac{\pi \Lambda^2 p_f^2}{9h^3 p} \times \left\{ \frac{4pp_f(p^2 - p_f^2 + \Lambda^2)}{[(p - p_f)^2 + \Lambda^2][(p + p_f)^2 + \Lambda^2]} - \log \left[\frac{(p + p_f)^2 + \Lambda^2}{(p - p_f)^2 + \Lambda^2} \right] \right\}. \quad (16)$$

The analytical forms of higher order symmetry potentials ($U_{sym,3}(\rho, p)$...) are not given because only the first order

and second order symmetry potentials ($U_{sym,1}(\rho, p)$ and $U_{sym,2}(\rho, p)$) are involved in determining the symmetry energy $E_{sym}(\rho)$ and its density slope $L(\rho)$.

Before we give the detailed results, it is interesting to compare both the isoscalar and isovector potentials of the MDI interaction with different x parameters. We show three typical cases of the MDI interaction with $x = -1, 0, \text{ and } 1$, respectively. The parameter x is very important because it determines the ratio of contributions of the density-dependent term in the MDI interaction to the total energy in the isospin singlet channel and triplet channel. For example, $x=1$ ($x=-1$) means that the density-dependent term contributes mostly to the $T=0$ ($T=1$) channel [3]. Thus, by varying x from -1 to 1, the MDI interaction covers a large range of uncertainties coming from the spin(isospin)-dependence of the in-medium many-body forces [3,51]. The parameter x does not affect the EOS of symmetric nuclear matter because the x related contributions from $T=0$ and $T=1$ channels can be cancelled out exactly [3]. In Fig.1, the momentum dependence of the $U_0(\rho, p)$, $U_{sym,1}(\rho, p)$, and $U_{sym,2}(\rho, p)$ is plotted at densities $0.5\rho_0$, ρ_0 , and $2\rho_0$, respectively. It is clearly seen in Fig.1 that the isoscalar potential $U_0(\rho, p)$ is increasing with the increasing momentum p while the $U_{sym,1}(\rho, p)$ and $U_{sym,2}(\rho, p)$ are all decreasing with the increasing momentum p . The $U_0(\rho, p)$ does not depend on the parameter x while both the $U_{sym,1}(\rho, p)$ and $U_{sym,2}(\rho, p)$ depend closely on the choice of parameter x . It is seen from Fig.1 that the first order symmetry potential $U_{sym,1}(\rho, p)$ varies significantly with different values of x . The only exception is the $U_{sym,1}(\rho, p)$ at the saturation density ρ_0 , which is independent of the choice of parameter x . This is not surprising because the symmetry energy $E_{sym}(\rho_0) =$

$\frac{1}{6} \frac{\partial[t+U_0]}{\partial k} \Big|_{k_F^0} \cdot k_F^0 + \frac{1}{2} U_{sym,1}(\rho_0, k_F^0)$ is fixed to be 30.55 MeV with any value of x at ρ_0 in the MDI interaction. Unlike the $U_{sym,1}(\rho, p)$, the second order symmetry potential $U_{sym,2}(\rho, p)$ is x -parameter dependent at all densities. Similar to the behavior of the $U_{sym,1}(\rho, p)$, the $U_{sym,2}(\rho, p)$ is also decreasing with the increasing momentum p in Fig.1. More importantly, it is found that the magnitude of $U_{sym,2}(\rho, p)$ becomes comparable to that of $U_{sym,1}(\rho, p)$ at high momentum ($p \geq 500$ MeV/c) or large density ($\rho = 2\rho_0$). Although the $U_{sym,2}$ term does not contribute to the symmetry energy $E_{sym}(\rho_0)$, however, its contribution to the slope parameter $L(\rho)$ is as large as $3U_{sym,2}(\rho, k_F)$ (see Eq.(12)). Thus the $U_{sym,2}$ term can not be neglected if its magnitude is comparable to that of $U_{sym,1}$.

In Fig.1, the $U_0(\rho, p)$, $U_{sym,1}(\rho, p)$ and $U_{sym,2}(\rho, p)$ have already shown a strong dependence on the density ρ . To show this density-dependence more clearly, we plot in Fig.2 the variation of both isoscalar and isovector potentials with the increasing density at the Fermi momentum ($p = p_f$). As pointed out in Ref.[4,28,29,30], it is the $U_{sym,1}(\rho, p_f)$ in Fig.2 responsible for the rather divergent density dependence of the symmetry energy $E_{sym}(\rho)$. For instance, with $x = 1$ the $U_{sym,1}$ term decreases very quickly with increasing density and thus results in a super-soft symmetry energy at supra saturation densities. On the contrary, the symmetry energy $E_{sym}(\rho)$ at supra saturation densities is very stiff for both $x = 0$ and $x = -1$ as the contribution of the $U_{sym,1}$ term becomes very positive with smaller values of x . The $U_{sym,2}(\rho, p)$ term does not contribute to the $E_{sym}(\rho)$ but do contribute to the density slope $L(\rho)$. One can see that the $U_{sym,2}$ is actually the most uncertain part and increases/decreases very fast with the density when the x parameter equals to $-1/1$. Thus the magnitude of $L(\rho)$ is expected to vary significantly with the x -parameter because of the $U_{sym,2}$ term contribution.

By using the analytical formulas of Eq.(9) and Eq.(12), the contribution of each term in the single-nucleon poten-

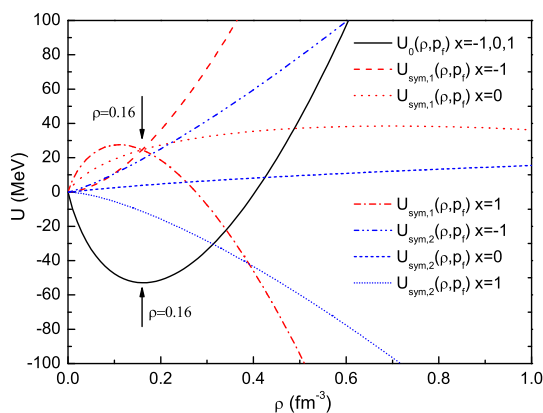


Fig. 2. Density dependence of the isoscalar and isovector potentials of the MDI interaction at $p = p_f$ with $x = -1, 0$, and 1 . The saturation density ρ_0 is denoted by the black arrows.

tial to the $E_{sym}(\rho)$ and $L(\rho)$ can be explicitly given. In Table 1 and Table 2, we list the contributions from the kinetic energy, U_0 , $U_{sym,1}$ and $U_{sym,2}$ to the $E_{sym}(\rho)$ and $L(\rho)$ at three different densities, respectively. As shown in the Tables 1 and 2, the kinetic energy and the U_0 term contributions to the $E_{sym}(\rho)$ and $L(\rho)$ are the same with different values of x , which increase smoothly with the increasing density. But the $U_{sym,1}$ term contribution varies largely with the choice of x -parameter at abnormal densities, which is clearly the key term in determining the density dependence of the $E_{sym}(\rho)$ (see Table 1). For the slope parameter $L(\rho)$, the $U_{sym,2}$ term becomes as important as the $U_{sym,1}$ term and contributes a large amount to the $L(\rho)$ (see Table 2). Unlike the kinetic energy and the U_0 term, the contribution of the $U_{sym,1}$ and $U_{sym,2}$ could be either positive or negative depending on the choice of the x -parameter.

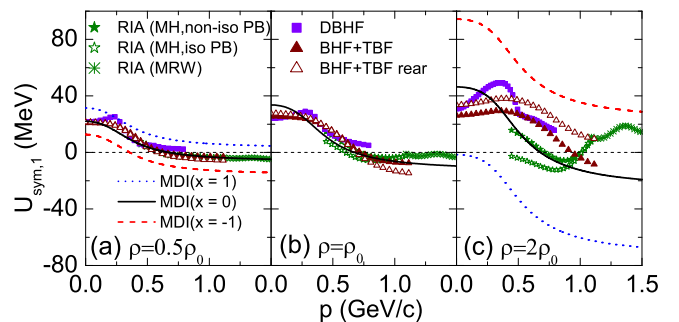


Fig. 3. Momentum dependence of the $U_{sym,1}(\rho, k)$ at $\rho = 0.5\rho_0$ (a), ρ_0 (b) and $2\rho_0$ (c) using the MDI interaction with $x = -1, 0$, and 1 . The corresponding results from several microscopic approaches are also included for comparison (Taken from Ref.[5]).

In Fig. 3, the first order symmetry potential $U_{sym,1}$ of the MDI interaction is compared with those from several microscopic approaches, which include the relativistic impulse approximation (RIA) [36,52,53,54], the relativistic Dirac-Brueckner-Hartree-Fock (DBHF) theory [55], and the non-relativistic Brueckner-Hartree-Fock (BHF) theory with/without the 3-body force (TBF) rearrangement contribution [56]. For these microscopic results, it is seen that they are consistent with each other below and around ρ_0 . However, there are still larger uncertainties at higher density of $\rho = 2\rho_0$. It is interesting to see that the momentum dependence of the $U_{sym,1}(\rho, k)$ from the MDI interaction with $x = 0$ agrees well with the results from the microscopic approaches. As mentioned above, the momentum dependence of the $U_{sym,1}(\rho, k)$ at ρ_0 is the same for $x = -1, 0$, and 1 because $U_{sym,1}(\rho, k)$ is independent of the x parameter at saturation density ρ_0 . In Fig. 4, the second-order symmetry potential $U_{sym,2}$ of the MDI interaction is compared with that from the Gogny Hartree-Fock approach. From Fig. 4, it is interesting to see that all these interactions firstly decrease with the momentum and then saturate when the momentum becomes larger than about 500 MeV/c. Especially the results of the MDI

Table 1. Contributions of different terms in the single-nucleon potential to the symmetry energy $E_{sym}(\rho)$ at densities $0.5\rho_0$, $1.0\rho_0$, and $2.0\rho_0$.

| Density | x parameter | kinetic energy contribution | U_0 term contribution | $U_{sym,1}$ term contribution | $U_{sym,2}$ term contribution | Total |
|--------------------|-------------|-----------------------------|-------------------------|-------------------------------|-------------------------------|-----------|
| $\rho = 0.5\rho_0$ | -1 | 7.74 | 2.94 | 3.67 | 0 | 14.35 MeV |
| | 0 | 7.74 | 2.94 | 8.38 | 0 | 19.06 MeV |
| | 1 | 7.74 | 2.94 | 13.08 | 0 | 23.76 MeV |
| $\rho = 1.0\rho_0$ | -1 | 12.29 | 5.96 | 12.30 | 0 | 30.55 MeV |
| | 0 | 12.29 | 5.96 | 12.30 | 0 | 30.55 MeV |
| | 1 | 12.29 | 5.96 | 12.30 | 0 | 30.55 MeV |
| $\rho = 2.0\rho_0$ | -1 | 19.52 | 11.29 | 40.20 | 0 | 71.01 MeV |
| | 0 | 19.52 | 11.29 | 16.51 | 0 | 47.32 MeV |
| | 1 | 19.52 | 11.29 | -7.18 | 0 | 23.63 MeV |

Table 2. Contributions of different terms in the single-nucleon potential to the density slope $L(\rho)$ at densities $0.5\rho_0$, $1.0\rho_0$, and $2.0\rho_0$.

| Density | x parameter | kinetic energy contribution | U_0 term contribution | $U_{sym,1}$ term contribution | $U_{sym,2}$ term contribution | Total |
|--------------------|-------------|-----------------------------|-------------------------|-------------------------------|-------------------------------|-------------|
| $\rho = 0.5\rho_0$ | -1 | 15.49 | 3.26 | 1.15 | 24.28 | 44.18 MeV |
| | 0 | 15.49 | 3.26 | 15.25 | 6.20 | 40.20 MeV |
| | 1 | 15.49 | 3.26 | 29.35 | -11.89 | 36.21 MeV |
| $\rho = 1.0\rho_0$ | -1 | 24.59 | 5.69 | 18.34 | 57.22 | 105.84 MeV |
| | 0 | 24.59 | 5.69 | 18.34 | 11.64 | 60.26 MeV |
| | 1 | 24.59 | 5.69 | 18.34 | -33.93 | 14.69 MeV |
| $\rho = 2.0\rho_0$ | -1 | 39.03 | 9.20 | 87.96 | 135.35 | 271.54 MeV |
| | 0 | 39.03 | 9.20 | 16.88 | 20.49 | 85.60 MeV |
| | 1 | 39.03 | 9.20 | -54.20 | -94.35 | -100.32 MeV |

interaction with $x = 1$ seem to be in reasonable agreement with those from the Gogny Hartree-Fock approach.

4 The optical model analysis of the single-nucleon potential and the corresponding symmetry energy and its density slope

The reliable information about the momentum/density dependence of single-nucleon potential (U_0 , $U_{sym,1}$ and $U_{sym,2}$) in asymmetric nuclear matter is essential to determine both the symmetry energy and its density slope. Note that the momentum/density dependence of the isoscalar potential U_0 around ρ_0 has been extensively investigated and relatively well constrained [57,58], although there is some uncertainties at high momentum/density. At the saturation density, the information on U_0 can be obtained from the energy dependence of the Global Optical Potential (GOP). Significant progress has been made in developing the unified GOP for both nuclear structure and reaction studies over the last several decades [59,60,61]. The GOP at negative energies can be constrained by single-nucleon energies of bound states while at positive energies it is constrained by nuclear reaction data [59,60,61]. The widely-used expression of the isoscalar potential is obtained from a large number of analysis of experimen-

tal scattering data and microscopic calculations [59]

$$U_0(\rho_0, E) = -(50.0 - 0.30E), \quad (17)$$

which gives an effective mass of $m^*/m = 0.7$ and a correct extrapolation value of $U_0 \simeq -54$ MeV at saturation density ($E = -16$ MeV), as required by the HVH theorem. Very recently, a new set of the global isospin dependent neutron-nucleus optical model potential parameters which include the symmetry potential up to the second order is obtained for the first time using the available experimental data from neutron-nucleus scatterings [6]. Shown in Fig. 5 is the energy dependence of the single-nucleon isoscalar potential U_0 obtained in Ref.[6]. For comparison, the results of the Schrödinger equivalent potential obtained by Hama *et al* [62] from the nucleon-nucleus scattering data are also shown. It is seen clearly that the isoscalar potential in Ref.[6] is in good agreement with that from the Hama's results.

The first order symmetry potential $U_{sym,1}$ can also be deduced from the optical potential [59,60] using a) elastic scattering of a neutron and a proton from the same target; b) proton scattering with the same beam energy on an isotopic chain; c) (p, n) charge exchange reaction between isobaric analog states. Since the 1960s, there are several sets of GOPs deduced from phenomenological model analyses of the available experimental data [63,64,65,66,67,68,69,70,71,72]. While some of the analyses assumed an energy independent symmetry potential, see, *e.g.*, [59,69,

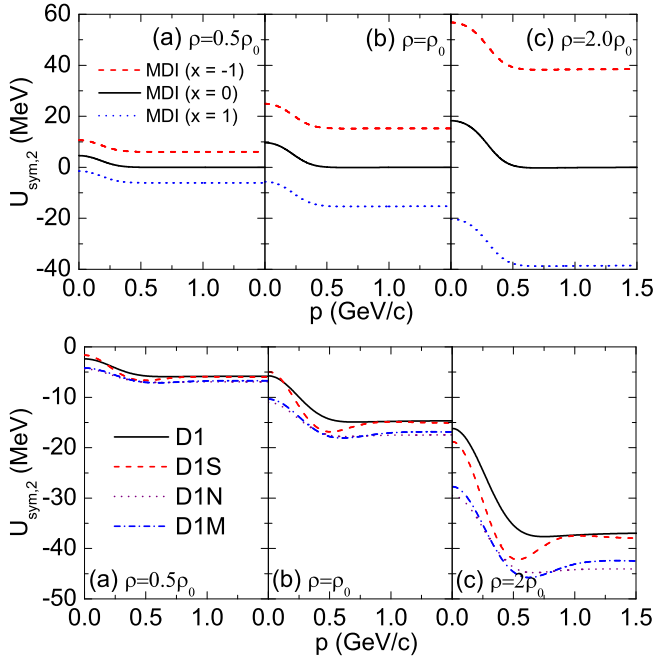


Fig. 4. Momentum dependence of the $U_{sym,2}(\rho, k)$ at $\rho = 0.5\rho_0$ (a), ρ_0 (b) and $2\rho_0$ (c) using the MDI interaction with $x = -1, 0$, and 1 and the Gogny Hartree-Fock approach with D1, D1S, D1N, and D1M (Taken from Ref.[5]).

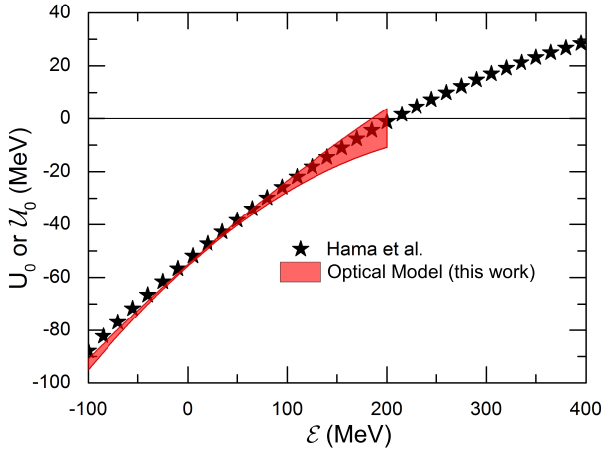


Fig. 5. Energy dependence of the isoscalar potential U_0 from the optical model analysis. The results of the Schrödinger equivalent potential obtained by Hama *et al* [62] from the nucleon-nucleus scattering data are also included for comparison (Taken from Ref.[6]).

70,71,72], a significant number of studies considered the energy dependence [63,64,65,66,67,68]. In these analyses the symmetry potentials are usually described by using a linear form $U_{sym,1}(\rho_0, E) = a_{sym} - b_{sym}E$. Assuming that these various global energy dependent symmetry potentials are equally accurate with the same predicting power beyond the original energy ranges in which they were studied, an averaged symmetry potential

$$U_{sym,1}(\rho_0, E) = 22.75 - 0.21E \quad (18)$$

was obtained [1], which represents the best fit to the global symmetry potentials constrained by the experimental data up to date. With this $U_{sym,1}$ and the isoscalar potential U_0 in Eq.(17), then the constraints $E_{sym}(\rho_0) = 31.3 \pm 4.5$ MeV and $L(\rho_0) = 52.7 \pm 22.5$ MeV were obtained simultaneously by neglecting the contribution of the second order symmetry potential to $L(\rho_0)$ [1].

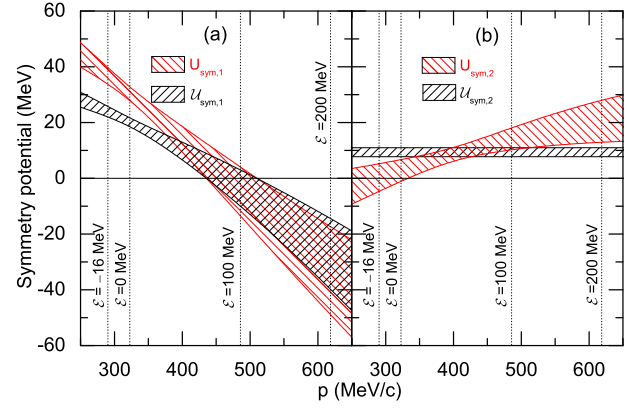


Fig. 6. Momentum dependence of the $U_{sym,1}$ (a) and $U_{sym,2}$ (b). The corresponding momenta at $\mathcal{E} = -16, 0, 100$ and 200 MeV are indicated by dotted lines. The $U_{sym,1}$ and $U_{sym,2}$ are terms in the real part of the central potential of the optical model (Taken from Ref.[6]).

In contrast to the first order symmetry potential $U_{sym,1}$, there is very few empirical/experimental information on the second order symmetry potential $U_{sym,2}$ [5,6]. In the usual optical model analyses, only the Lane potential $U_{sym,1}$ has been considered. It is thus of great importance to extract experimental information about the $U_{sym,2}$ and examine its effects on the density slope of the symmetry energy. Here we show the information on both the $U_{sym,1}$ and $U_{sym,2}$ from the very recent optical model analysis of available experimental data [6]. Shown in Fig. 6 is the momentum dependence of both the $U_{sym,1}$ and $U_{sym,2}$ from the optical model studies. It is seen that the $U_{sym,1}$ decreases with momentum p and becomes negative when the momentum is larger than about $p = 470$ MeV/c (i.e., $\mathcal{E} = 90$ MeV). On the contrary, it is interesting to see that the $U_{sym,2}$ increases with the nucleon momentum p . It is also seen that the $U_{sym,2}$ essentially vanishes around $\mathcal{E} = -16$ MeV, as shown in Fig. 6. Thus the contribution of the $U_{sym,2}$ term is very small to the density slope $L(\rho)$ at ρ_0 , though with a large uncertainty [6], verifying the assumption made in Ref.[1]. The new optical model analysis leads to a value of $E_{sym}(\rho_0) = 37.24 \pm 2.26$ MeV and $L(\rho_0) = 44.98 \pm 22.31$ MeV, consistent with the results obtained from analyzing many other observables within various models.

5 Summary

In summary, the general relationship between the symmetry energy and the single-nucleon potential in isospin-

asymmetric matter was derived by using the Hugenholtz-Van Hove theorem. Both the symmetry energy $E_{sym}(\rho)$ and its density slope $L(\rho)$ can be expressed explicitly in terms of the magnitude and momentum dependence of the nucleon isoscalar and isovector potential in asymmetric nuclear matter. These analytical formulas are useful for extracting reliable information about the EOS of neutron-rich nuclear matter from experimental data. Using the isospin and momentum dependent MDI interaction model as an example, the contributions of different terms in the single-nucleon potential (MDI) to the $E_{sym}(\rho)$ and $L(\rho)$ are analyzed in detail for different densities. The first-order symmetry potential is found to be responsible for the uncertain high density behavior of the $E_{sym}(\rho)$ while the density slope $L(\rho)$ depend on both the first-order and second-order symmetry potentials. By using the derived analytical formulas and the single-nucleon potentials from the optical model analysis, both the symmetry energy $E_{sym}(\rho)$ and its density slope $L(\rho)$ at the saturation density ρ_0 were extracted. To further constrain the $L(\rho)$ at high densities, more reliable information about the second-order symmetry potential $U_{sym,2}$ is useful.

Acknowledgments

The authors would like to thank Bao-Jun Cai, Rong Chen, and Xiao-Hua Li for fruitful collaboration and stimulating discussions. This work is supported by the National Natural Science Foundation of China (Grant Nos 11175085, 11235001, 11035001, 11135011, and 11275125), by the Project Funded by the Priority Academic Program Development of Jiangsu Higher Education Institutions (PAPD), by the Shanghai Rising-Star Program under grant No. 11QH1401100, the ‘‘Shu Guang’’ project supported by Shanghai Municipal Education Commission and Shanghai Education Development Foundation, the Program for Professor of Special Appointment (Eastern Scholar) at Shanghai Institutions of Higher Learning, the Science and Technology Commission of Shanghai Municipality (11DZ2260700), and by the US National Aeronautics and Space Administration under grant NNX11AC41G issued through the Science Mission Directorate, the US National Science Foundation under Grant No. PHY-1068022 and the CUSTIPEN (China-U.S. Theory Institute for Physics with Exotic Nuclei) under DOE grant number DE-FG02-13ER42025.

References

1. C. Xu, B. A. Li, and L. W. Chen, Phys. Rev. C **82**, (2010) 054607.
2. C. Xu, B. A. Li, L. W. Chen, and C. M. Ko, Nucl. Phys. A **865**, 1 (2011).
3. C. Xu and B. A. Li, Phys. Rev. C **81**, (2010) 044603.
4. C. Xu and B. A. Li, Phys. Rev. C **81**, (2010) 064612.
5. R. Chen, B.J. Cai, L.W. Chen, B.A. Li, X.H. Li, and C. Xu, Phys. Rev. C **85**, (2012) 024305.
6. X. H. Li, B. J. Cai, L. W. Chen, R. Chen, B. A. Li, and C. Xu, Phys. Lett. B **721**, (2013) 101.
7. B. A. Li, C. M. Ko and W. Bauer, Int. Jour. Mod. Phys. E **7**, (1998) 147.
8. B. A. Li, L. W. Chen and C. M. Ko, Phys. Rep. **464**, (2008) 113.
9. Isospin Physics in Heavy-Ion Collisions at Intermediate Energies, Eds. Bao-An Li and W. Udo Schröer (Nova Science Publishers, Inc, New York, 2001).
10. J. M. Lattimer, M. Prakash, Science **304**, (2004) 536.
11. A. W. Steiner, M. Prakash, J. M. Lattimer, P. J. Ellis, Phys. Rep. **411**, (2005) 325.
12. P. Danielewicz, R. Lacey and W. G. Lynch, Science **298**, (2002) 1592.
13. P. J. Siemens, Nucl. Phys. A **141**, (1970) 225.
14. C. -H. Lee, T. T. Kuo, G. Q. Li, and G. E. Brown, Phys. Rev. C **57**, (1998) 3488.
15. A. W. Steiner, Phys. Rev. C **74**, (2006) 045808.
16. O. Sjöberg, Nucl. Phys. A **222**, (1974) 161.
17. B. A. Brown, Phys. Rev. Lett. **85**, (2000) 5296.
18. V. Baran, M. Colonna, V. Greco, M. Di Toro, Phys. Rep. **410**, (2005) 335.
19. M. Di Toro, V. Baran, M. Colonna and V. Greco, J. Phys. G: Nucl. Part. Phys. **37**, (2010) 083101.
20. K. Sumiyoshi and H. Toki, Astrophys. J. **422**, (1994) 700.
21. I. Bombaci, Chapter 2 in Ref.[9].
22. L. W. Chen, C. M. Ko and B. A. Li, Phys. Rev. Lett. **94**, (2005) 032701.
23. B. A. Li and L. W. Chen, Phys. Rev. C **72**, (2005) 064611.
24. M. B. Tsang, Yingxun Zhang, P. Danielewicz, M. Famiano, Zhuxia Li, W. G. Lynch, and A. W. Steiner, Phys. Rev. Lett. **102**, (2009) 122701.
25. M. Centelles, X. Roca-Maza, X. Vinas and M. Warda, Phys. Rev. Lett. **102**, (2009) 122502.
26. J. B. Natowitz et al., Phys. Rev. Lett. **104**, 202501 (2010).
27. Z. G. Xiao, B. A. Li, L. W. Chen, G. C. Yong and M. Zhang, Phys. Rev. Lett. **102**, (2009) 062502.
28. C. B. Das, S. Das Gupta, C. Gale, B. A. Li, Phys. Rev. C **67**, (2003) 034611.
29. B. A. Li, C. B. Das, S. Das Gupta, C. Gale, Phys. Rev. C **69**, (2004) 011603 (R).
30. B. A. Li, C. B. Das, S. Das Gupta, C. Gale, Nucl. Phys. A **735**, (2004) 563.
31. S. Ulrych and H. Müther, Phys. Rev. C **56**, (1997) 1788.
32. E. N. E. van Dalen, C. Fuchs, and A. Faessler, Nucl. Phys. A **74**, (2004) 227.
33. W. Zuo, L. G. Cao, B. A. Li, U. Lombardo, and C. W. Shen, Phys. Rev. C **72**, (2005) 014005.
34. S. Fritsch, N. Kaiser, W. Weise, Nucl. Phys. A **750**, (2005) 259.
35. J. A. McNeil, J. R. Shepard, S. J. Wallace, Phys. Rev. Lett. **50**, (1983) 1439.
36. L. W. Chen, C. M. Ko, B. A. Li, Phys. Rev. C **72**, (2005) 064606.
37. Z. H. Li, L. W. Chen, C. M. Ko, B. A. Li, and H. R. Ma, Phys. Rev. C **74**, (2006) 044613.
38. J. R. Stone, J. C. Miller, R. Koncewicz, P. D. Stevenson, M.R. Strayer, Phys. Rev. C **68**, (2003) 034324.
39. V. R. Pandharipande, V.K. Garde, Phys. Lett. B **39**, (1972) 608.
40. R. B. Wiringa et al., Phys. Rev. C **38**, (1988) 1010.
41. M. Kutschera, Phys. Lett. B **340**, (1994) 1.

42. Nuclear Density Functional Theory, Nuclear Structure Near the Limits of Stability (INT-05-3) September 26 to December 2, 2005
[http : //www.int.washington.edu/PROGRAMS/dft.html](http://www.int.washington.edu/PROGRAMS/dft.html)
43. B.J. Cai and L.W. Chen, Phys. Lett. B **711**, (2012) 104.
44. N. M. Hugenholtz and L. Van Hove, Physica **24**, (1958) 363.
45. L. Satpathy, V. S. Uma Maheswari and R. C. Nayak, Phys. Rep. **319**, (1999) 85.
46. K. A. Brueckner and J. Dabrowski, Phys. Rev. **134**, (1964) B722.
47. J. Dabrowski and P. Haensel, Phys. Lett. B **42**, (1972) 163.
48. J. Dabrowski and P. Haensel, Phys. Rev. C **7**, (1973) 916.
49. J. Dabrowski and P. Haensel, Can. J. Phys. **52**, (1974) 1768.
50. A. M. Lane, Nucl. Phys. **35**, (1962) 676.
51. J. Decharge and D. Gogny, Phys. Rev. C **21**, (1980) 1568.
52. Z. H. Li, L. W. Chen, C. M. Ko, B. A. Li, and H. R. Ma, Phys. Rev. C **74**, (2006) 044613.
53. D.P. Murdock and C. J. Horowitz, Phys. Rev. C **35**, (1987) 1442.
54. J. A. McNeil, L. Ray, and S.J. Wallace, Phys. Rev. C **27**, (1983) 2123.
55. E. N. E. van Dalen, C. Fuchs, and A. Faessler, Phys. Rev. C **72**, (2005) 065803.
56. W. Zuo, U. Lombardo, H.-J. Schulze, and Z.H. Li, Phys. Rev. C **74**, (2006) 014317.
57. M. A. Preston and R. K. Bhaduri, Structure of the Nucleus (Addison-Wesley, Reading, MA, 1975), p. 191-202.
58. G. F. Bertsch and S. Das Gupta, Phys. Rep. **160**, (1988) 189.
59. P. E. Hodgson, The Nucleon Optical Potential (World Scientific Publishing, Sigapore 1994) page 7.
60. G. R. Satchler, W. G. Love, Phys. Rep. **55**, 183 (1979).
61. C. Mahaux and R. Sartor, Advances in Nuclear Physics, Vol. 20, Ed. J.W. Negele and E. Vogt (New York, Plenum), pp 1-223 (1991).
62. S. Hama, B. C. Clark, E. D. Cooper, H. S. Sherif, and R. L. Mercer, Phys. Rev. C **41**, (1990) 2737.
63. A. J. Koning et al., Nucl. Phys. A **713**, (2003) 231.
64. J.-P. Jeukenne et al., Phys. Rev. C **43**, (1991) 2211.
65. J. Rapaport et al., Nucl. Phys. A **330**, (1979) 15.
66. R. P. De Vito *et. al.*, NSCL/MSU report-363, (1981).
67. K. Kwiatkowski et al., Nucl. Phys. A **301**, (1978) 349.
68. D. M. Patterson *et. al.*, Nucl. Phys. A **263**,(1976) 261.
69. Y. L. Han *et. al.*, Phys. Rev. C **81**, (2010) 024616.
70. O. V. Bessalova et al., J. Phys. G **29**, (2003) 1193.
71. R. L. Varner *et al.*, Phys. Rep. **201**, (1991) 57.
72. F. D. Becchetti and G. W. Greenlees Phys. Rev. **182**, (1969) 1190.